Theoretical Analysis of Intermolecular Covalent $\pi-\pi$ Bonding and Magnetic Properties of Phenalenyl and *spiro*-Biphenalenyl Radical π-Dimers

Jingsong Huang*,† and Miklos Kertesz*

Department of Chemistry, Georgetown University, 37th and O Street, Washington, DC 20057-1227

Received: March 15, 2007; In Final Form: May 3, 2007

Singlet−triplet splittings ΔE_{ST} and intermolecular covalent $\pi-\pi$ bonding characteristics of the prototypical phenalenyl π-dimer and eight *spiro*-biphenalenyl radical π-dimer structures are analyzed with the aid of restricted and unrestricted density functional theory calculations and paramagnetic susceptibility data fitted using the Bleaney−Bowers dimer model and the Curie−Weiss model. Single determinant approximations for ΔE_{ST} as a function of transfer integrals and on-site Coulomb repulsion energy are presented for the two-electron two-site π-dimers of phenalenyls and the two-electron four-site π-dimers of *spiro*-biphenalenyl radicals. Within the range of intermolecular separation of $3.12 < D < 3.51$ Å, for the shorter separations, restricted theory works quite well and indicates the presence of a relatively strong intermolecular covalent $\pi-\pi$ bonding interaction. For the longer separations, the singlet−triplet splittings are small; electron correlation plays a significant role, and only the unrestricted theory provides results that are in qualitative agreement with experiments. The bonding interactions in the π-dimers are gradually weakened with increasing D, showing a transition from low D values with significant intermolecular $\pi-\pi$ bonding and electron delocalization to high D values with localized spins and a biradicaloid character.

1. Introduction

Organic molecular crystals of neutral π-radicals are exciting because of their potentials as molecular metals.[1] Phenalenyl (**1**) is an organic neutral radical with an unpaired electron in the singly occupied molecular orbital (SOMO;[1] Chart 1). Because of the large delocalized domain of the SOMO electron, **1** is stable in solution as indicated by electron spin resonance (ESR), but it undergoes σ-dimerization in the solid state (Scheme 1).[2,3] Substitution with bulky *tert*-butyl groups leads to a π-dimerization in the solid state for 2,5,8-tri-*tert*-butylphenalenyl radical, **2** (Scheme 1).[4] ESR, UV−vis, and MS also confirm the π-dimerization of **2** in solutions and even in the gas phase.[5,6] The overlap between the two SOMOs is effective in the staggered conformation shown in Scheme 1, bottom right.

The intermolecular separation D in the π-dimer of **2** is about 3.2−3.3 Å,[4] slightly shorter than the sum of the van der Waals (vdW) radii, indicating the presence of attractive intermolecular multicenter covalent $\pi-\pi$ bonding interaction.[4,6,7] This bonding is enhanced if all six of the spin-bearing C centers participate in the bonding interaction. When the overlap is favorable as for **2**, the strength of such $\pi-\pi$ bonding interaction is on the order of ca. 9 kcal/mol,[6] which is only slightly weaker than the σ-bond in the σ-dimer of **1** by 1−5 kcal/mol.[3,8] Such intermolecular covalent $\pi-\pi$ bonding exists not only for neutral radicals[9] but also for charged π-radicals[10] such as tetracyanoethylene dimer dianion, $[TCNE]_2^{2-}$,[9,11] and oligothiophene π-dimer dication.[12] Similarly interesting are closed shell π-trimers,[13] which will not be addressed here, however. The common feature of these radical π-dimers and trimers is their sub-vdW intermolecular separation.

CHART 1: Phenalenyl Radical (1) and Its SOMO

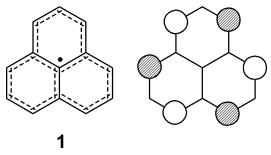

1

SCHEME 1: σ-Dimerization of Phenalenyl Radical (1) and π-Dimerization of 2,5,8-Tri-*tert*-butylphenalenyl Radical (2)[a]

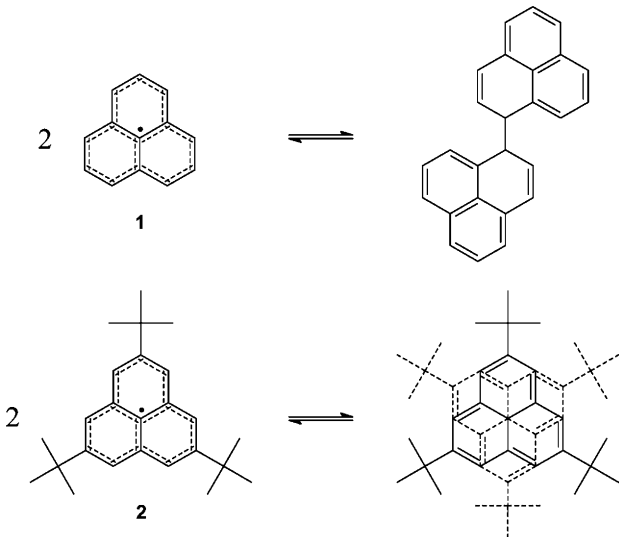

[a] Note the inversion center in the π-dimer at the bottom right.

Haddon et al. have recently reported a series of *spiro*-biphenalenyl (SBP) radicals, **3**−**10** (Chart 2),[14−20] each consisting of two nearly perpendicular phenalenyl units interacting through a boron spiro-linkage. In these neutral radicals, one of

* To whom correspondence should be addressed. Tel: 202-687-5761. Fax: 202-687-6209. E-mail: kertesz@georgetown.edu.
† Current address: Oak Ridge National Laboratory, Bethel Valley Road, Oak Ridge, TN 37831-6367. E-mail: huangj3@ornl.gov.

10.1021/jp072086p CCC: $37.00
Published on Web 06/26/2007

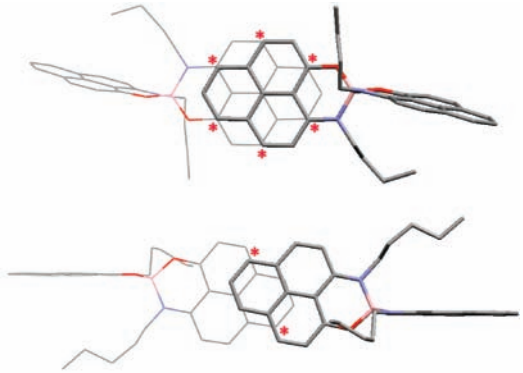

Figure 1. π-Dimers of butyl-SBP (**5**, top) and pentyl-SBP (**6**, bottom) with six pairs and two pairs of spin-bearing C overlaps, respectively, as indicated by the red asterisks. Hydrogens are left out for clarity.

CHART 2: SBP Neutral Radicals with Various Substitutions

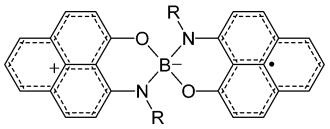

3. R = Ethyl
4. R = Propyl
5. R = Butyl
6. R = Pentyl
7. R = Hexyl
8. R = Benzyl
9. R = Octyl
10. R = Cyclohexyl

the two phenalenyl SOMO electrons fills into the atomic orbital (AO) of the electron-deficient boron atom, leaving one unpaired electron in the frontier molecular orbital (MO). These SBPs exhibit diverse packing motifs in the solid state depending on the substituents. Unlike **1** and **2**, hexyl-SBP (**7**) remains monomeric, and its magnetic properties indicate that **7** behaves as a free radical with one spin per molecule.[17] Benzyl-SBP (**8**) aggregates in the solid state into a quasi one-dimensional (1D) π-step stack. The overlap between neighboring molecules is favorable only for one out of the six spin-bearing C atoms per phenalenyl unit.[18] The magnetic properties of **8** were interpreted by an antiferromagnetic Heisenberg $S = 1/2$ linear chain model.[18] The rest of the SBP radicals, excluding cyclohexyl-SBP (**10**), form π-dimers similar to **2**. The π-dimers of ethyl- (**3**), propyl- (**4**), butyl- (**5**), and octyl-SBPs (**9**) involve six pairs of intermolecular C−C overlap, with intermolecular distances ranging from 3.12 to 3.40 Å,[14,15,19,21] while the π-dimer of pentyl-SBP (**6**) has only two pairs of intermolecular C−C overlap and the intermolecular separation at 3.51 Å is a bit larger accordingly.[16] Two SBP π-dimers are illustrated in Figure 1. For **10**, neighboring molecules adopt similar π-dimer stacking as in **2**−**5** and **9** using six overlapping pairs of spin-bearing C atoms; furthermore, intermolecular multicenter $\pi-\pi$ overlap of **10** with both left and right neighbors leads to quasi 1D π-chain along which the intermolecular separation between phenalenyl rings is 3.28 Å.[20] Theoretical calculations indicate that the good intermolecular $\pi-\pi$ overlap leads to a large bandwidth W and efficient electron delocalization along the π-chain of **10** providing a pathway for unusually high electrical conduction for this purely organic neutral radical material.[22]

In this paper, we focus on π-dimerization among the three kinds of π-type aggregates (π-step, π-dimer, and π-chain) of the SBP radicals. Some of the intermolecular separations in the π-dimers **3**−**6** and **9** are slightly shorter than the sum of the vdW radii similar to the π-dimer of **2**, implying additional attractive covalent $\pi-\pi$ bonding on the top of vdW forces. Multicenter covalent $\pi-\pi$ bonding has been characterized by MO theory[7] and by structural[4] and spectroscopic measurements[4−6] for **2** but not for the SBP radicals. Because chemical bonding and magnetism often go hand-in-hand,[23] it is also important to investigate theoretically the magnetic properties of these π-dimerized SBP radicals to gain insight into the structural and bonding characteristics of these π-radicals. To make the story complete for the π-radicals **3**−**6** and **9**, we also studied theoretically the π-dimer of **2** from the perspective of magnetism and compared the obtained results with the available magnetic (ESR and SQUID) and spectroscopic data for **2**. Our density functional theory (DFT) calculations indicate that the stacked π-radicals **2**, **3**, **5**, and **9** are bound tighter together due to multicenter covalent $\pi-\pi$ bonding interactions.

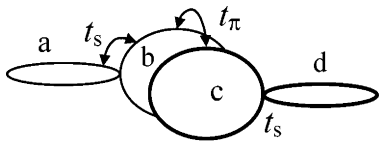

Figure 2. Schematic of a π-dimer of SBP neutral radicals; each molecule is represented by two joint ellipses indicating spiro-conjugation at the boron atom (see Chart 2). The four phenalenyl units are denoted as sites a, b, c, and d. The transfer integrals, t_s and t_π, characterize the intramolecular spiro-conjugation (between a and b and between c and d) and the intermolecular $\pi-\pi$ overlap (between b and c), respectively.

2. Theoretical Framework

We followed a two-pronged approach. We performed first principles all-electron DFT calculations to obtain realistic parameters to be compared with experimental data. The Computational Methods section contains the relevant technical details. Electron correlation is an essential feature of the interactions of two radicals; the consideration of electron correlation beyond the restricted MO theory is necessary to understand the nature of intermolecular interactions in these π-dimers. Therefore, we supplemented these DFT calculations with analysis based on MO theory and the Hubbard dimer model. The Hubbard model is completely defined by the Coulomb repulsion parameter U and the transfer integral t.[24] Each phenalenyl unit is represented by one site in the model, with a Hubbard on-site Coulomb repulsion energy U, corresponding to the Coulomb repulsion energy between two electrons localized on one site. The Hubbard transfer integrals are of two different kinds: One represents the $\pi-\pi$ interaction (t_π), and the other, in the case of SBPs, corresponds to the spiro-conjugation interaction (t_s). Therefore, the dimer of **2** corresponds to two sites (t_s is absent), and the dimers of the SBPs (**3**−**6** and **9**) correspond to four sites shown in Figure 2. The number of SOMO electrons is two in both cases; thus, the dimer of **2** corresponds to half filling, while the dimers of SBPs correspond to quarter filling. The energy difference ΔE_{ST} between the ground singlet state and the low-lying excited triplet state can be qualitatively analyzed on the basis of these two radical electrons in the π-dimers.

2.1. Restricted MO Theory and Single Configuration Approximation. Our discussion is presented on the basis of symmetry-adapted MOs.[25,26] We confine ourselves first to the restricted MO theory level, and then, we consider the inclusion of electron correlation. This strategy allows us to discern when restricted MO theory is a good approximation and when correlation plays a significant role.

With the assumption that the π-radicals are bound together, at least partially, by multicenter covalent $\pi-\pi$ bonding interaction in the π-dimers, MO theory is applied as follows to these dimer systems. As shown earlier,[4b,6,7] two sets of monomer orbitals overlap in the π-dimers to give a set of dimer orbitals.

For the materials in this study, the monomer radical SOMOs are isolated in energy from the rest of the MOs and play a dominant role in the formation of π-dimers; therefore, we focus first on the SOMO-related dimer orbitals as the active orbitals. The overlap of the two SOMOs produces an orbital with in-phase orbital interaction and another with out-of-phase orbital interaction. The highest occupied molecular orbital (HOMO) and lowest unoccupied molecular orbital (LUMO) of the dimers are indexed as 1 and 2, respectively. The wave functions of the dimer HOMO and LUMO are ψ_1 and ψ_2. Assuming an inversion center, the dimer HOMOs and LUMOs have a_u and a_g symmetry, respectively. Their energies are ϵ_1 and ϵ_2, and the dimer HOMO−LUMO splitting ($\epsilon_2 - \epsilon_1$) reflects the strength of the $\pi-\pi$ covalent bonding (non-vdW) part of the intermolecular interactions.

Depending on the occupancy of the dimer HOMO and LUMO, there are six basic Slater determinants shown in Figure 3. The correct symmetry-adapted combinations replace ψ_D and ψ_E:

$$\psi_{D'} = \frac{1}{\sqrt{2}}(\psi_D + \psi_E) \tag{1}$$

and

$$\psi_{E'} = \frac{1}{\sqrt{2}}(\psi_D - \psi_E) \tag{2}$$

The energies of these determinants can be expressed in terms of the one-electron energy h_i, Coulomb integral J_{ij}, and exchange integral K_{ij} using the notation of Szabo and Ostlund:[27]

$$h_i = \langle\psi_A|\hat{f}_i|\psi_A\rangle;\ J_{12} = \langle\psi_1(1)\psi_2(2)|\hat{g}_{12}|\psi_1(1)\psi_2(2)\rangle;\ \text{etc.} \tag{3}$$

Assuming that the dimer HOMO and LUMO energies are constant for the six determinants shown in Figure 3, we can replace the h_i terms in the energy expressions with the orbital energies, ϵ_1 and ϵ_2, where[27]

$$\epsilon_1 = h_1 + J_{11} \tag{4}$$

and

$$\epsilon_2 = h_2 + 2J_{12} - K_{12} \tag{5}$$

Thus, we obtain four energy values corresponding to four configurations. The energy of the ground singlet configuration S_0 (ψ_A) is

$$E_{S_0} = 2h_1 + J_{11} = 2\epsilon_1 - J_{11} \tag{6}$$

The energy of the low-lying excited triplet configuration T (ψ_B, ψ_C, and $\psi_{D'}$) is

$$E_T = h_1 + h_2 + J_{12} - K_{12} = \epsilon_1 + \epsilon_2 - J_{11} - J_{12} \tag{7}$$

The energy of the excited singlet configuration S_1 ($\psi_{E'}$) is

$$E_{S_1} = h_1 + h_2 + J_{12} + K_{12} = \epsilon_1 + \epsilon_2 - J_{11} - J_{12} + 2K_{12} \tag{8}$$

The energy of the third singlet configuration S_2 (ψ_F) is

$$E_{S_2} = 2h_2 + J_{22} = 2\epsilon_2 - 4J_{12} + 2K_{12} + J_{22} \tag{9}$$

The symmetry species of these four configurations are ^1A_g, ^3A_u, ^1A_u, and ^1A_g, respectively.[28]

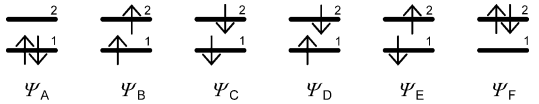

Figure 3. Six Slater determinants $\psi_A-\psi_F$ of radical π-dimers indicating the occupancy of the phenalenyl SOMO-derived dimer HOMO and LUMO with indices 1 and 2, respectively. For the four-site cases (dimers of **3**−**6** and **9**), there are two further higher lying dimer orbitals derived from phenalenyl SOMOs (see Figure 4).

The singlet−triplet splitting in this single configuration approximation is

$$\Delta E_{ST} = E_{S_0} - E_T = \epsilon_1 - \epsilon_2 + J_{12} \tag{10}$$

which is associated with the $S_0 \rightarrow T$ transition and can be observed indirectly through the paramagnetic component of the magnetic susceptibility. ΔE_{ST} is negative when the triplet is above the singlet. ΔE_{ST} is on the order of −0.3 eV for **2** from ESR measurements.[29] The S_2 configuration also has an effect on ΔE_{ST}: In the case of very weak $\pi-\pi$ bonding interactions, the dimer HOMO−LUMO splitting ($\epsilon_2 - \epsilon_1$) is small and one has to go beyond the single configuration approximation, for example, by using configuration interaction (CI), to obtain the correct energies of the weakly bonded π-dimers. In fact, among the four configurations, only the mixing between S_0 and S_2 is possible by symmetry. Such admixture of the doubly excited configuration ψ_F into the singlet ground state ψ_A leads to a biradicaloid character,[30] for which a broken-symmetry approach[7,31] can be employed instead of CI to address the correlation effects.

When ΔE_{ST} is positive, then the triplet is below the singlet and it becomes the ground state (spin crossover). This situation may occur when the dimer level splitting is small as compared to the exchange term,

$$\epsilon_2 - \epsilon_1 < J_{12} \tag{11}$$

However, in general, the single configuration approximation becomes less accurate when ($\epsilon_2 - \epsilon_1$) is small. Consequently, when such a situation arises, the single configuration approach can only indicate but not prove the presence of such a spin crossover. We shall show that all of the π-dimers in this study have singlet ground state even in the case when the $\pi-\pi$ bonding interaction is very weak.

The $S_0 \rightarrow S_1$ transition is characteristic of radical π-dimers and is usually termed the charge transfer (CT) transition, ΔE_{CT},[32,33] which reflects the transfer of one radical electron from a monomer to its neighboring molecule in the π-dimer. The corresponding energy difference, ΔE_{CT}, is on the order of the on-site Coulomb repulsion energy U.[34] This transition is observable by UV−vis and is not our concern in this paper. We shall focus on the $S_0 \rightarrow T$ transition observable through magnetic susceptibility, because the ΔE_{ST} value can be a measure of the covalent $\pi-\pi$ bonding strength.[35]

We now turn to the two-electron two-site and four-site theoretical models to obtain approximate relationships for ΔE_{ST}, U, and the transfer integrals t_π (t_s), which will be useful in the analysis of the all-electron DFT calculations on the dimers of **2**−**6** and **9**.

2.2. ΔE_{ST} for Two-Site Systems. First, we investigate the π-dimer of **2** consisting of two phenalenyl units that are coupled

by the transfer integral t_π. The secular equation of a two-site system is

$$\begin{vmatrix} -\epsilon & t_\pi \\ t_\pi & -\epsilon \end{vmatrix} = 0 \tag{12}$$

where ϵ represents the dimer orbital energies and t_π is the transfer integral due to $\pi-\pi$ overlap. We define the electronic interaction through $\pi-\pi$ overlap of the two π-stacked phenalenyls by the out-of-phase orbital combination so that t_π is positive. Solving eq 12, we obtain the HOMO and LUMO as

$$\psi_1 = \frac{1}{\sqrt{2}}(\phi_a + \phi_b) \text{ and } \psi_2 = \frac{1}{\sqrt{2}}(\phi_a - \phi_b) \tag{13}$$

where ϕ_a and ϕ_b are the local SOMO orbitals. The energies of the HOMO and LUMO are

$$\epsilon_1 = -t_\pi \text{ and } \epsilon_2 = t_\pi \tag{14}$$

Equation 10 becomes

$$\Delta E_{ST} = -2t_\pi + J_{12} \tag{15}$$

Substituting eq 13 into the expression of the Coulomb integral J_{12} gives

$$J_{12} = \left\langle \psi_1(1)\psi_1(1)\left|\frac{1}{r_{12}}\right|\psi_2(2)\psi_2(2)\right\rangle \approx \frac{1}{4}[(\phi_a\phi_a|\phi_a\phi_a) + (\phi_b\phi_b|\phi_b\phi_b)] = \frac{1}{2}(\phi_a\phi_a|\phi_a\phi_a) \tag{16}$$

where we keep only on-site Coulomb integrals using the Hubbard model for the on-site Coulomb repulsion U, which leads to the following in the single configuration approximation

$$\Delta E_{ST} = -2t_\pi + \frac{U}{2} \tag{17}$$

Next, we show that this MO-based derivation is consistent with the Hubbard model containing a transfer integral t and an on-site Coulomb repulsion U in terms of energies. The exact solution to ΔE_{ST} within the Hubbard model is[32,36,37]

$$\Delta E_{ST} = \frac{U}{2} - C = \frac{U}{2} - \sqrt{4t^2 + \left(\frac{U}{2}\right)^2} \tag{18}$$

In the limit of large $4t/U$, using Taylor expansion, $C \approx 2t$.

The physical meaning of $4t$ is the bandwidth W of a 1D chain of sites. At the large $4t/U$ limit, this is a weakly correlated system, that is, $U \ll W$.[38] Therefore,

$$-2t + \frac{U}{2} = \Delta E_{ST} < 0 \tag{19}$$

This indicates that in the weakly correlated limit, MO theory is a good approximation, and the π-dimers can be described as being bonded by intermolecular covalent $\pi-\pi$ bonding. We shall use DFT to calculate ΔE_{ST} for the covalent $\pi-\pi$ bonded systems. As we can see later, the MO approximation breaks down in case of weakly bonded (strongly correlated) π-dimers, and correlation plays an important role. Under such circumstances, we go beyond MO theory and perform broken-symmetry unrestricted (U) DFT calculations.[7,31]

2.3. ΔE_{ST} for Four-Site Systems. Next, we turn to the SBP π-dimers consisting of four phenalenyl units. These can be represented as four-site systems as shown in Figure 2. The local SOMO wave functions of the four phenalenyl sites a−d are ϕ_a, ϕ_b, ϕ_c, and ϕ_d, respectively.

Because of the C_i symmetry of the π-dimers, we construct the symmetry-adapted linear combinations of these site orbitals as follows.

$$\phi_1 = \frac{1}{\sqrt{2}}(\phi_a + \phi_d) \tag{20}$$

$$\phi_2 = \frac{1}{\sqrt{2}}(\phi_b + \phi_c) \tag{21}$$

$$\phi_3 = \frac{1}{\sqrt{2}}(\phi_a - \phi_d) \tag{22}$$

$$\phi_4 = \frac{1}{\sqrt{2}}(\phi_b - \phi_c) \tag{23}$$

The plus combinations are associated with a_u symmetry, and the minus combinations are associated with a_g symmetry. We define the electronic transfer integrals through spiro-conjugation and $\pi-\pi$ overlap by the out-of-phase combinations of the adjacent phenalenyl moieties so that both t_s and t_π are positive.[22a] The matrix elements of the secular equation are

$$H_{11} = \frac{1}{2}(\langle\phi_a|\hat{H}|\phi_a\rangle + \langle\phi_d|\hat{H}|\phi_d\rangle + \langle\phi_a|\hat{H}|\phi_d\rangle + \langle\phi_d|\hat{H}|\phi_a\rangle) = \alpha \tag{24}$$

$$H_{12} = H_{21} = \frac{1}{2}(\langle\phi_a|\hat{H}|\phi_b\rangle + \langle\phi_a|\hat{H}|\phi_c\rangle + \langle\phi_d|\hat{H}|\phi_b\rangle + \langle\phi_d|\hat{H}|\phi_c\rangle) = -t_s \tag{25}$$

$$H_{22} = \frac{1}{2}(\langle\phi_b|\hat{H}|\phi_b\rangle + \langle\phi_c|\hat{H}|\phi_c\rangle + \langle\phi_b|\hat{H}|\phi_c\rangle + \langle\phi_c|\hat{H}|\phi_b\rangle) = \alpha - t_\pi \tag{26}$$

$$H_{33} = \frac{1}{2}(\langle\phi_a|\hat{H}|\phi_a\rangle + \langle\phi_d|\hat{H}|\phi_d\rangle - \langle\phi_a|\hat{H}|\phi_d\rangle - \langle\phi_d|\hat{H}|\phi_a\rangle) = \alpha \tag{27}$$

$$H_{34} = H_{43} = \frac{1}{2}(\langle\phi_a|\hat{H}|\phi_b\rangle - \langle\phi_a|\hat{H}|\phi_c\rangle - \langle\phi_d|\hat{H}|\phi_b\rangle + \langle\phi_d|\hat{H}|\phi_c\rangle) = -t_s \tag{28}$$

$$H_{44} = \frac{1}{2}(\langle\phi_b|\hat{H}|\phi_b\rangle + \langle\phi_c|\hat{H}|\phi_c\rangle - \langle\phi_b|\hat{H}|\phi_c\rangle - \langle\phi_c|\hat{H}|\phi_b\rangle) = \alpha + t_\pi \tag{29}$$

Setting $\alpha = 0$, the secular equation is

$$\begin{vmatrix} -\epsilon & -t_s & 0 & 0 \\ -t_s & -\epsilon - t_\pi & 0 & 0 \\ 0 & 0 & -\epsilon & -t_s \\ 0 & 0 & -t_s & -\epsilon + t_\pi \end{vmatrix} = 0 \tag{30}$$

The solutions to the above equation are, in the order of increasing energies:

$$\epsilon_1(a_u) = \frac{-t_\pi - \sqrt{t_\pi^2 + 4t_s^2}}{2} \quad (31)$$

$$\epsilon_2(a_g) = \frac{t_\pi - \sqrt{t_\pi^2 + 4t_s^2}}{2} \quad (32)$$

$$\epsilon_3(a_u) = \frac{-t_\pi + \sqrt{t_\pi^2 + 4t_s^2}}{2} \quad (33)$$

$$\epsilon_4(a_g) = \frac{t_\pi + \sqrt{t_\pi^2 + 4t_s^2}}{2} \quad (34)$$

These four energy levels are shown in Figure 4. The energy differences of $(\epsilon_2 - \epsilon_1)$ and $(\epsilon_4 - \epsilon_3)$ are equal to t_π. This derivation is based on the assumption that the overlaps $S_{ij} = 0$ for $i \neq j$. These small overlaps are not completely negligible, and they are partially responsible for the fact that in the actual DFT calculations the values of $(\epsilon_2 - \epsilon_1)$ and $(\epsilon_4 - \epsilon_3)$ are different. We will take the average of these two values to calculate t_π. With the value of t_π so obtained, t_s can be solved by using the $(\epsilon_3 - \epsilon_1)$ or $(\epsilon_4 - \epsilon_2)$.

Assuming that the two SOMO electrons occupy only the lowest two levels shown in Figures 3 and 4, we arrive at the same four single configurations as shown in eqs 6−9. In the single configuration approximation, eq 10 becomes now

$$\Delta E_{ST} = -t_\pi + J_{12} \quad (35)$$

As we will see later, the value of t_π depends on the intermolecular separations in the SBP radical π-dimers, while the values of t_s are more or less constant across the family of SBPs. Therefore, the coefficients of ϕ_a through ϕ_d in ψ_1 and ψ_2 depend on the relative magnitudes of t_s and t_π. Accordingly, unlike eq 17 for a two-site system, the J_{12} term in eq 35 is not constant and it depends on the t_π/t_s ratio leading to the following relationship

$$\Delta E_{ST} \approx -t_\pi + \frac{U}{[4 + (t_\pi/t_s)^2]} \quad (36)$$

Equation 36 is derived similar to eq 17 where we keep only the on-site Coulomb integrals. This approximation strongly influences the value of J_{12}. Nevertheless, we shall see that the estimated value of U for the four-site SBP π-dimers based on eq 36 is consistent with that from the two-site π-dimer of **2**.

3. Computational Details

Molecular calculations were performed with the Gaussian 03 program.[39] The π-dimer **2** (Scheme 1) was excised from the X-ray crystal structure of **2**,[4] and the geometry was used in a dimer calculation without further geometry optimization. This dimer approach is justified by the crystal packing of **2** showing that the neighboring π-dimers are well-separated and nearly perpendicular to each other, leading to very small overlap between π-dimers. This dimer approach was also employed for the calculations of the π-dimers of **3**−**6** and **9**, since the neighboring π-dimers of the SBP radicals are also nearly perpendicular to each other, similar to the crystal packing of **2**. Total energy and transfer integral calculations using these dimer X-ray structures are described below in detail.

Single-point total energy calculations were performed for both the singlet ground state and the low-lying excited triplet state for **2**−**6** and **9** to obtain ΔE_{ST} values. Several density functionals were tested for **2**, including nonhybrid PW91,[40] BLYP,[41] and hybrid B3LYP.[42] By comparing these results with the experimental data of **2**, we chose the B3LYP density functional to calculate total energies of the π-dimers of **3**−**6** and **9**. To account for electron correlation effect, we employed more affordable broken-symmetry unrestricted[7,31] UDFT calculations. For the initial guess, the HOMO and LUMO are mixed to lift the spatial symmetries, thus producing unrestricted wave functions for singlet states. Wave function stability analysis[43] was performed on the restricted singlet wave functions obtained from the RB3LYP single-point calculations on the π-dimers of **3**−**6** and **9** to further check the UDFT results.

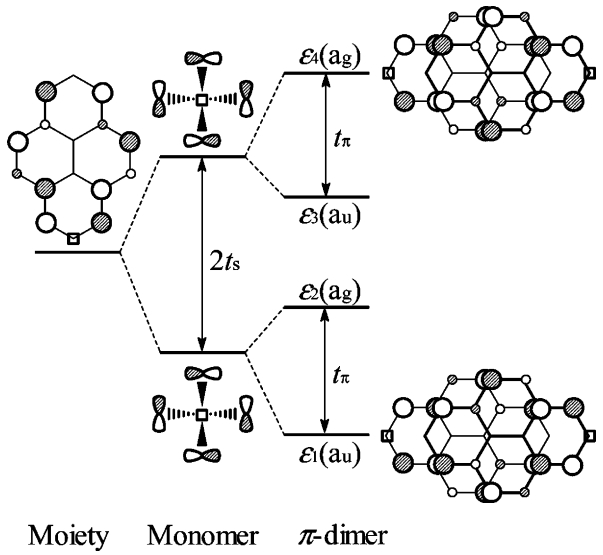

Figure 4. Development of the four SOMO-derived π-dimer orbitals starting from the half-SBP moiety as a result of spiro-conjugation (monomer) and $\pi-\pi$ overlap (π-dimer). Orbital splittings are expressed in terms of transfer integrals t_s and t_π. Boron atoms (□) are at the center of spiro-conjugation; substituents are omitted. Top views of the first and the fourth dimer orbitals are shown; the second is similar to the fourth one, and the third is similar to the first one, except for the spiro-conjugation.

We also took an alternative approach to calculate ΔE_{ST} for the π-dimer of **2**. Solid-state calculations were performed for the three-dimensional (3D) X-ray crystal structure of **2** using the plane wave based Vienna ab initio simulation package (VASP).[44] The singlet and triplet states were obtained by different NUPDOWN parameters, which specify the difference between the numbers of electrons with up and down spins. We used a $4 \times 4 \times 4$ k-mesh.

To investigate the dependence of ΔE_{ST} on t_π for the π-dimer of **2** shown in eq 17, transfer integrals are calculated for a series of staggered π-dimers of **1** with the same staggered packing as that of **2** shown in Scheme 1. Interplanar separation D of the π-dimers of **1** is in the range of 3.0−4.0 Å. The bond distances of C−C and C−H in **1** are fixed to 1.40 and 1.08 Å, respectively.[7] All bond angles are fixed to 120°, and each phenalenyl is completely planar. Calculations for **2** refer to the experimental D value. Using these π-dimer geometries, transfer integrals t_π were calculated from half of the dimer HOMO−LUMO level splitting (eq 14) obtained from the single-point calculations of the ground singlet states. Unlike the total energy calculations using B3LYP density functional, a different density functional, PW91, was used for the transfer integral calculations. This theory has been validated in our earlier work for organic molecular materials.[45] This methodology validated for **1** and **2** is then applied to the SBP π-dimers **3**−**6** and **9** to study the $\Delta E_{ST}-t_\pi$ correlation for four-site systems shown in eq 36.

TABLE 1: Comparison of ΔE_{ST} for the π-Dimers of 2 from DFT and Hartree−Fock (HF) Calculations with Experiments

theory	A_x[a]	ΔE_{ST} (eV)
	RDFT	
RPW91[b]	0	−0.573
RPW91[c]	0	−0.569[d]
RBLYP	0	−0.592[d]
RB3LYP	0.2	−0.353[d]
	UDFT and UHF	
UBLYP	0	−0.580[e] (−0.592)[f]
UB3LYP	0.2	−0.376[e] (−0.383)[f]
UB2LYP	0.5	−0.237[e]
UHF	1	−0.155[e]

experiments	ΔE_{ST} (eV)
SQUID[g]	−0.17
ESR[h]	−0.288

[a] A_x is the amount of exact exchange used. [b] Solid-state calculations using plane-wave basis set. [c] This and the rest are dimer calculations. [d] 6-31G* basis set. [e] From ref 7, 6-31G basis set. [f] This work, 6-31G*. [g] Ref 4. [h] −6.64 kcal/mol, ref 29.

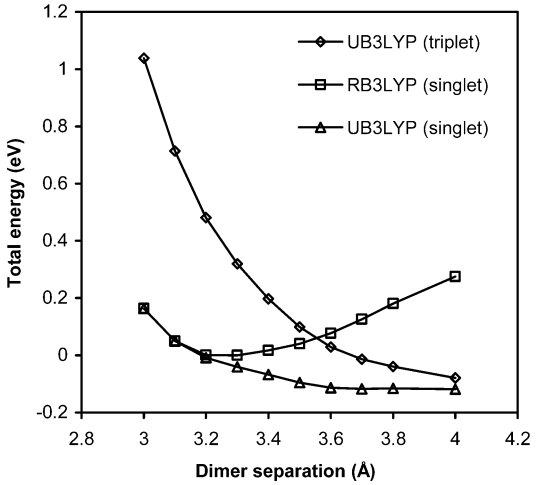

Figure 5. Total energies calculated with R(U)B3LYP/6-31G* for the π-dimers of **1** relative to that of the RB3LYP singlet at 3.3 Å. The bifurcation point of the two singlet curves is at 3.2 Å.

Transfer integrals t_π and t_s are calculated from the four SOMO-related orbital energies using eqs 31−34. t_π was approximated as $(\epsilon_2 - \epsilon_1 + \epsilon_4 - \epsilon_3)/2$. This t_π value was substituted back into $(\epsilon_3 - \epsilon_1)$ and $(\epsilon_4 - \epsilon_2)$, and then, the average value was taken to obtain the transfer integral t_s.

According to our earlier basis set convergence study on transfer integrals,[46] we used the 6-31G* basis set for the molecular calculations and a plane-wave basis set with kinetic energy cutoff of 286.7 eV for the solid-state calculations, which have been shown to be sufficient for organic compounds containing first-row atoms.[46]

4. Results and Discussions

4.1. Two-Site Systems. We calculated the ΔE_{ST} with both restricted (R) and unrestricted (U) DFT for the π-dimers of **2**, and the results are tabulated in Table 1 together with those obtained from SQUID and ESR measurements. Some theoretical results from ref 7 calculated with a smaller basis set (6-31G) are also included for comparison.

First, we compare the calculations performed on the 3D crystal and the π-dimer of **2** using RPW91 density functional. The value of ΔE_{ST} for the 3D crystal calculation using a plane-wave basis set is in good agreement with that calculated from the π-dimer excised from the unit cell using a 6-31G* Gaussian basis set. This good agreement justifies the dimer approach. The dimer approach is also corroborated by the band structure showing very small dispersion, which is therefore not presented here. The small dispersion of the bands points to negligible interdimer interactions. The rest of the calculations are performed on the π-dimers excised from the unit cell of **2**.

RB3LYP provides a smaller ΔE_{ST} value than RPW91. This can be ascribed to the fact that B3LYP contains 20% exact exchange ($A_x = 0.2$; see Table 1) in the exchange-correlation functional. The unrestricted UDFT and UHF results of Takano et al. shown in Table 1 indicate a trend that with higher degree of HF exchange included, the magnitude of ΔE_{ST} is smaller.[7] It has been shown that HF often overestimates the relative stability of the high spin state.[47] In comparison, calculations with RBLYP give ΔE_{ST} comparable to those of RPW91 since both are nonhybrid density functionals ($A_x = 0$).

Comparing the restricted RDFT results with the unrestricted ones, we can see that the unrestricted UB3LYP result has a slightly larger ΔE_{ST}. As we discussed in the theoretical framework section, in situations when the dimer $\pi-\pi$ bonding interactions are weak, the mixing of the S_0 and S_2 configurations cannot be neglected and electron correlation plays an important role. Unrestricted UDFT includes some of this mixing; therefore, the total energy of the lowest singlet is slightly lowered. This is illustrated in Figure 5 using the staggered π-dimers of **1**, which has the same packing motif as the π-dimer of **2**. Figure 5 shows that the UB3LYP ground singlet state energy is the same as the RB3LYP singlet value when the intermolecular separation is small, that is, when the bonding interaction is strong. However, the UB3LYP singlet curve diverges from the RB3LYP singlet curve at a Coulson−Fisher bifurcation point, which in this case is around 3.2 Å. On the right side of the bifurcation point, the UB3LYP singlet energies are lower than the RB3LYP singlet energies as a result of electron correlation. This behavior is very similar to the potential energy curves of the ground singlet state of H_2 molecule.[27] Although there is a crossover between RB3LYP singlet curve and UB3LYP triplet curve at ca. 3.55 Å, with UB3LYP, the singlet energies are always lower than the triplet energies. In comparison, ΔE_{ST} obtained from UBLYP is the same as that from RBLYP for the experimental geometry of the π-dimer of **2**. (Note that BLYP is a nonhybrid density functional and thus $A_x = 0$.) We found that the corresponding bifurcation point with BLYP is at a rather large intermolecular separation of 3.6 Å. The actual intermolecular separation of 3.2−3.3 Å of the π-dimer of **2** is close to the bifurcation point at 3.2 Å shown in Figure 5, explaining the slight difference of the ΔE_{ST} values between the restricted and the unrestricted B3LYP calculations in Table 1. Because this difference is small, we conclude that the restricted level of theory is a good approximation for the π-dimer of **2**, and the single configurations offer a qualitatively correct description using ψ_A for S_0 and any one of the triplet configurations ψ_B, ψ_C, and ψ_D, for T. Therefore, the two radicals in the π-dimer of **2** can be described as being held together by intermolecular covalent $\pi-\pi$ bonding interaction.

Comparison between the theoretically calculated ΔE_{ST} with the experimental results from ESR measurements shown in Table 1 indicates that B3LYP and B2LYP hybrid density functionals provide the best agreement with experiment among the theories shown. Earlier SQUID measured ΔE_{ST} is much lower than that of the later ESR measurement, which is generally more sensitive than SQUID. B3LYP theory has been widely used for ΔE_{ST} calculations, giving good agreement with post-

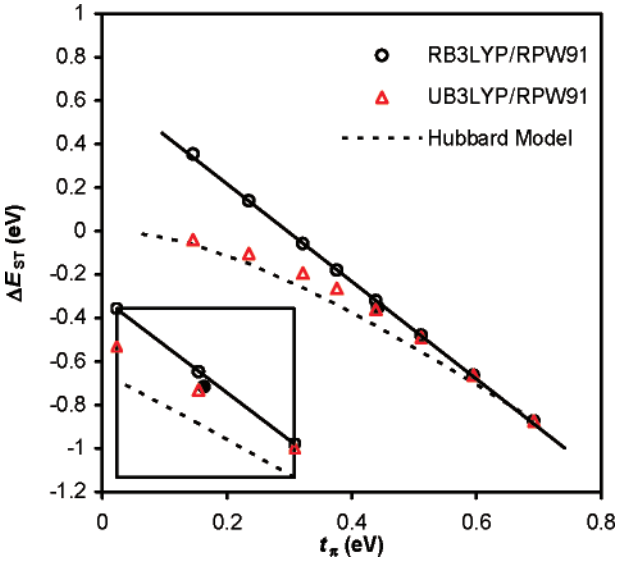

Figure 6. Correlation diagram of ΔE_{ST} vs t_π for the staggered π-dimers of **1** (empty symbols) and the staggered π-dimer of **2** (filled symbol, only at the experimental geometry; see the inset for an enlarged view) calculated by the B3LYP/PW91 approach, which refers to a combination of B3LYP for ΔE_{ST} and PW91for t_π. The straight line shows the best linear fit with $\Delta E_{ST} = -2.245\ t_\pi + 0.667$ ($R^2 = 0.9991$). The ideal linear relationship for single determinant approximation is $\Delta E_{ST} = -2\ t_\pi + U/2$; see eq 17.

HF correlation calculations and with experiments for a variety of organic molecules.[48] We will see that it provides good agreement with experimental values from paramagnetism measurements for the SBP radical π-dimers as well. For the π-dimer of **2**, ΔE_{ST} is -6.64 kcal/mol from ESR and is -8.14 kcal/mol from RB3LYP calculations. We can compare these values with the dimer binding energy, ΔE_D, defined as the energy difference between the π-dimer and the two well-separated monomer radicals. The dimer binding energies have been measured for **2** by ESR and UV−vis, and the values are -9.5 and -8.8 kcal/mol, respectively.[6] Michl pointed out that the $S_0 \rightarrow S_1$ energy difference is related to the energy for heterolytic dissociation and the $S_0 \rightarrow T$ transition is linked to the chemical bonding strength, that is, the energy for homolytic dissociation, which is reflected by the dimer binding energy ΔE_D.[49] It turns out that the ΔE_{ST} and ΔE_D values for **2** are comparable, indicating the covalent $\pi-\pi$ bonding strength is on the order of 7−10 kcal/mol. This bonding strength is only slightly weaker than the σ-bond in the σ-dimer shown in Scheme 1,[3,8] which is surprising in the sense that the intermolecular separation, if it can be called a "$\pi-\pi$ bond length," is almost twice as long as the σ-bond length. Our earlier study shows that such $\pi-\pi$ bonding effect is significant, leading to an unusual $\pi-\pi$ bonded intermediate in the Cope rearrangement of a *cyclo*-biphenalenyl.[50] It is also the driving force of the unusual four-center two-electron CC bonds with very long distance of 2.8 Å in the TCNE dimer dianion.[11]

Next, we examine the correlation between ΔE_{ST} and t_π shown in eq 17. To control the transfer integral, we considered π-dimers of **1** with variable intermolecular separation, D. The corresponding data are plotted in Figure 6, together with the data for the π-dimer of **2** at the experimental D. For the reliable calculations of intermolecular transfer integrals, one can use a nonhybrid DFT in combination with either sufficiently large Gaussian basis sets or plane-wave basis sets.[45,46] Meanwhile, the reliable calculations of ΔE_{ST} require the B3LYP hybrid density functional.[48] As we have mentioned before, the PW91 density functional overestimates the ΔE_{ST} values while B3LYP overestimates the transfer integrals.[45] A better approach is therefore obtained by using B3LYP to calculate the ΔE_{ST} and using PW91 to calculate the transfer integrals, and this approach is termed the B3LYP/PW91 combination. The $\Delta E_{ST}-t_\pi$ correlation obtained in this way is shown in Figure 6 with ΔE_{ST} and t_π calculated by R(U)B3LYP and RPW91, respectively. First, let us look at the RB3LYP/RPW91 results. The data point of the π-dimer **2** is very close to the results of **1**, showing that the *tert*-butyl groups do not affect the $\Delta E_{ST}-t_\pi$ correlation significantly. The data points of the π-dimers **1** can be well-described by a linear fit with a slope of ca. -2, in good agreement with eq 17. The intercept ($U/2$) of the linear fit for the RB3LYP/RPW91 combination provides a value of on-site Coulomb repulsion energy $U = 1.3$ eV, which is in good qualitative agreement with those obtained from electrochemistry.[51] This U value is on the order of 1 eV for π-radicals,[32−34] and it varies slightly depending on which phenalenyl moiety it corresponds to. The redox potential difference for phenalenyl and the singly reduced phenalenyl anion are 1.6 V,[52] leading to the estimate of $U = 1.6$ eV for **1**. The U value of **2** is ca. 1.5 eV.[4a] Derivatives of phenalenyl tend to have smaller U values, due to the increased domain available for delocalization of the electrons and the reduced electron−electron repulsion in their anions. The experimental U values of the perchloro-phenalenyl radical and the perchloro-2,5,8-triazaphenalenyl radical are 1.22 and 1.35 eV.[53] In comparison, the RB3LYP/RB3LYP or RPW91/RPW91 combinations produce on-site U values of 2.4 and 0.6 eV, respectively, which do not agree as well with the U values from electrochemistry, even though the slopes of their linear fits are close to -2 (-1.902 and -1.994, respectively). Note that the theoretical U values are only expected to correlate with but not to agree with those obtained from electrochemistry in solution.

The dashed curve in Figure 6 was obtained from the Hubbard dimer model shown in eq 18 with $U = 1.3$ eV. Within the exact Hubbard model, ΔE_{ST} is always negative with the decreasing t_π, as opposed to the RB3LYP calculations. However, this trend is well-reproduced with UB3LYP/RPW91 calculations as shown in Figure 6 since UB3LYP calculations include some electron correlation. In any case, with increasing t_π, the restricted or unrestricted B3LYP calculations and the Hubbard model gradually converge, showing that restricted MO is a good approximation and electron correlation is less important. This should hold true for the π-dimer of **2**, indicating once again that the MO theory is a good approximation and the two phenalenyl radicals are bound together by intermolecular covalent $\pi-\pi$ bonding interaction.

4.2. Four-Site Systems. In the following, we examine the five π-dimerized SBP radicals. The magnetic susceptibilities have been measured using a Faraday balance by Haddon et al.[14−19] The paramagnetic susceptibilities χ_p are obtained by subtracting diamagnetic susceptibilities using Pascal's Law[54] and are collected in Figure 7 as a function of temperature T. Propyl-, pentyl-, and octyl-SBPs each show a maximum at $T_{max} = 34$, 29, and 28 K, respectively, which is a signature of antiferromagnetic interaction.[26] Below T_{max}, χ_p decreases with decreasing T, but rises up again at low temperature (<10 K; see Figure 8 for detail). The χ_p values of ethyl- and butyl-SBPs exhibit a jump at $T = 130-150$ and 320−350 K, respectively, corresponding to the phase transition of the two materials. The χ_p curve of butyl-SBP further exhibits hysteresis at its phase transition temperature. It is apparent that these χ_p values, except that of octyl-SBP, tend to the same value of ~0.001 emu mol^{-1}

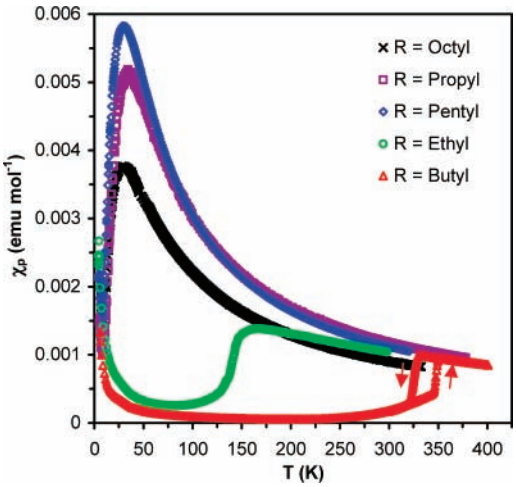

Figure 7. Paramagnetic susceptibility χ_p of the π-dimers of the five SBP neutral radicals as a function of temperature T. Arrows show the hysteresis of the butyl-SBP radical. Experimental data are from refs 14a, 15, 16, and 19.

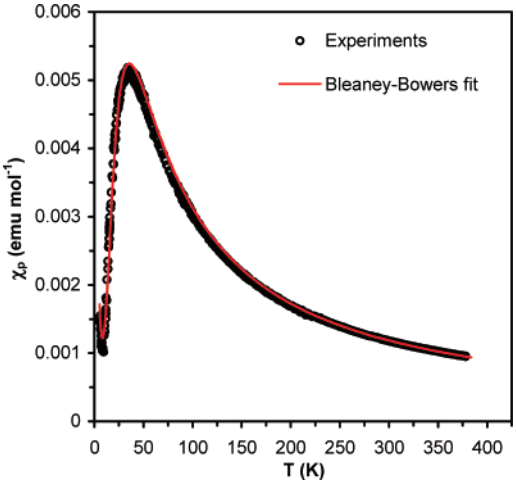

Figure 8. Two-parameter Bleaney−Bowers dimer model fit for the π-dimer of propyl-SBP neutral radical. Experimental data are from ref 15.

at around 350 K. This χ_p value gives a χ_pT value of ~0.35 emu K mol^{-1}. This experimental limiting χ_pT value is close to but still lower than 3/8 emu K mol^{-1}, which is the ideal χ_pT value at high T for spins with $S = 1/2$.

The strength of the interaction between the two π-radical spins is characterized by the value of ΔE_{ST}, which can be extracted by an analysis based on the Bleaney−Bowers dimer model together with a consideration for the paramagnetic contributions from P percent impurity often following Curie law at low temperature:[26,55]

$$\chi_p(T) = \frac{N_A g^2 \mu_B{}^2}{k_B T[3 + \exp(-\Delta E_{ST}/k_B T)]}(1 - P) + \frac{N_A g^2 \mu_B{}^2}{4k_B T} P \quad (37)$$

where N_A is Avogadro's number, g is the gyromagnetic factor, μ_B is the electronic Bohr magneton, and k_B is the Boltzmann constant. The results of such an analysis are illustrated in Figure 8, which shows a two-parameter fit (ΔE_{ST} and P) performed with the SigmaPlot program for the data from propyl-SBP.[15] The impurity term is necessary to account for the rising χ_p values

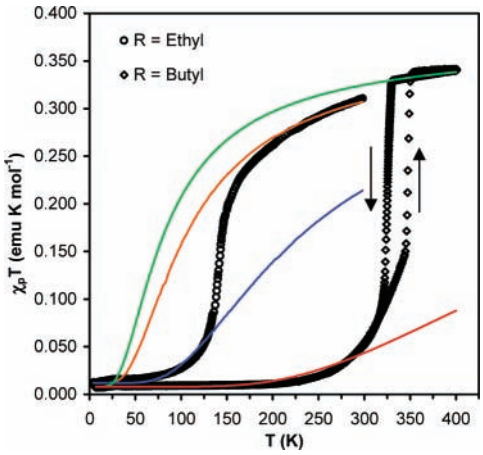

Figure 9. Two-parameter Bleaney−Bowers dimer model fit for ethyl- and butyl-SBPs for both low-T phases and high-T phases. Experimental data are from ref 14a.

below 10 K. The same fit can be applied to pentyl- and octyl-SBP as well. The analyses for the ethyl- and butyl-SBP radical dimers are performed for both low-T and high-T phases (Figure 9). As one can see from Figure 9, even at $T = 400$ K, the value of χ_pT is still lower than the ideal value of 3/8 emu K mol^{-1}. The dimer model fitting parameters are collected in Table 2. The goodness of fit indicates that the Bleaney−Bowers dimer model instead of the tetramer model[56] is applicable because there are only two spins even though the π-dimers have four sites.

An alternative, albeit less precise analysis, is provided by the application of a Curie−Weiss fit:

$$\chi_p = \frac{C}{T - \theta} \quad (38)$$

where θ is the Weiss temperature. A negative θ indicates an antiferromagnetic interaction, and a positive θ indicates a ferromagnetic one. This is exemplified with propyl-SBP, and the high-T phases of ethyl- and butyl-SBPs shown in Figure 10 and Table 2. The analysis for the low-T phases of ethyl- and butyl-SBPs is not performed because of impurities. All of the negative θ values for the π-dimers show that the interactions between the π-radicals have antiferromagnetic characteristics. It is worth pointing out that although the sign of θ provides information about the intermolecular interaction (ferromagnetic or antiferromagnetic), the magnitude of ΔE_{ST} is a better indicator for bonding strength. By comparing the ΔE_{ST} values from Bleaney−Bowers dimer model fit and from theoretical calculations, we will be able to tell in what cases restricted MO theory is a good approximation and the two radicals are bound by covalent bonding interactions.

In Table 2, the π-dimers are arranged in the order of increasing D. The four ethyl-SBP structures were determined by Haddon et al. at four different temperatures: 20, 100, 173, and 293 K. The high-T phase structure of the butyl-SBP is not yet available in the literature. The trend of the Weiss temperatures is consistent with that of D, indicating stronger interactions between radicals at smaller D. This trend is also reflected in the ΔE_{ST} values obtained from the Bleaney−Bowers dimer model fit. The fit results are corroborated by the ΔE_{ST} values obtained from the T_{max} calculations by using the following equation.[26,57]

$$|\Delta E_{ST}| = 1.604kT_{max} \quad (39)$$

Note that for the high-T phases of ethyl- and butyl-SBPs, the T_{max} does not exist because of phase transition, but they are

TABLE 2: Comparison of the Curie−Weiss Fit Results and Bleaney−Bowers Dimer Model Fit Results with Theoretical Calculations Based on Restricted and Unrestricted B3LYP Calculations

							RB3LYP	UB3LYP	
dimers	D (Å)[a]	θ (K)	ΔE_{ST} (eV, from T_{max})[b]	ΔE_{ST} (eV, from Bleaney−Bowers)	R^2 of fit	impurity P (%)	ΔE_{ST} (eV)	ΔE_{ST} (eV)	$\langle S^2\rangle$ of singlet
butyl, **5** (low-T phase)	3.12			−0.094	0.994	2.1	−0.096	−0.135	0.521
ethyl, **3** (low-T phase)	3.16			−0.037	0.978	3.2	−0.014	−0.082	0.646
	3.18						−0.002	−0.076	0.669
ethyl, **3** (high-T phase)	3.31	−83[c,d]	−0.016	−0.017	0.974	3.2[e]	0.193	−0.019	0.928
	3.35						0.197	−0.018	0.993
butyl, **5** (high-T phase)		−46[c,d]	−0.012	−0.013	0.998	2.1[e]			
octyl, **9**	3.4	−37[f]	−0.004	−0.008	0.677	5.6	0.246	−0.013	0.972
propyl, **4**	3.40	−24[d]	−0.005	−0.005	0.994	2.4	0.227	−0.016	0.967
pentyl, **6**	3.51	−17[g]	−0.004	−0.004	0.990	3.0	0.415	−0.001	1.060

[a] D, interplanar separation from the X-ray structures (see refs 14a, 15, 16, and 19). [b] Using eq 39 and assuming that the impurity effect is small. There are no directly observed T_{max} values for the high-T phases of ethyl- and butyl-SBPs, but they are obtained from our Bleaney−Bowers fit. [c] Curie−Weiss fits for the high-T phases of the ethyl- and butyl-SBP structures. [d] Fit with a constraint of $C = 0.375$; the C values in pentyl- and octyl-SBPs are close to 0.375 from fittings without constraints (refs 16 and 19). [e] The impurities of high-T phases are constrained to be the same as those from low-T phases fit without constraint. [f] Ref 19. [g] Ref 16.

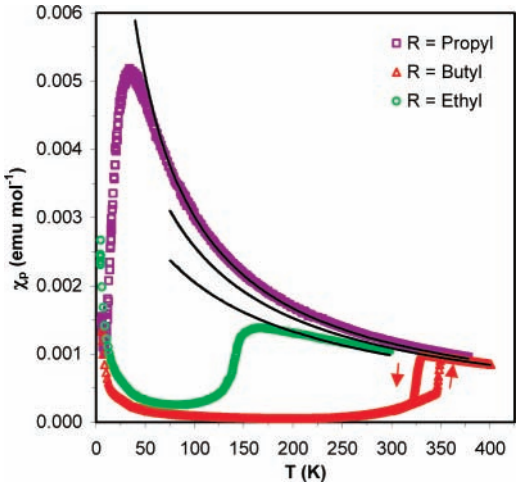

Figure 10. Curie−Weiss fit for propyl-SBP and the higher temperature phases of ethyl- and butyl-SBPs. Experimental data are from refs 14a and 15.

obtained based on the Bleaney−Bowers fit. That should be the reason why the agreement between the ΔE_{ST} values from the two approaches is so good for ethyl- and butyl-SBPs. Nevertheless, the agreement is excellent for propyl- and pentyl-SBPs, except for octyl-SBP where the goodness of Bleaney−Bowers fit, R^2, is much lower than for all of the other cases. This lower R^2 value of the Bleaney−Bowers fit for octyl-SBP may partially come from the larger amount of impurity. According to the trend of interaction strength shown in D, θ, and ΔE_{ST}, we can predict that the D of butyl-SBP radical π-dimer in the high-T phase should be somewhere between 3.35 and 3.40 Å.

Next, we compare the theoretical values of ΔE_{ST} with those from the Bleaney−Bowers fit. The ΔE_{ST} values were calculated using the π-dimers excised from the crystal structure without further geometry optimization. With RB3LYP, the ΔE_{ST} values are negative for the low-T phases of butyl- and ethyl-SBPs, indicating singlet ground states for these dimers. The RB3LYP ΔE_{ST} values are positive for the rest of the π-dimers, indicating a spin-crossover (triplet ground state) at this level of theory. However, experimental results based on the Bleaney−Bowers fit indicate otherwise with all ΔE_{ST} values being negative. To partially account for the S_0-S_2 mixing, we performed broken-symmetry unrestricted UB3LYP calculations for all π-dimers. For the low-T phase of the butyl-SBP, the UB3LYP result is only slightly lower than the RB3LYP result and both agree with the Bleaney−Bowers dimer model fit. Similar to the π-dimer case of **2**, the difference between RB3LYP and UB3LYP results for the low-T phase structure of butyl-SBP π-dimer is small, implying that the correlation effect is small, and single configuration MO is a good approximation. This is also the case for the low-T phase structures of the ethyl-SBP, albeit to a lesser degree. Starting from the high-T phase structures of the ethyl-SBP, UB3LYP calculations provide negative ΔE_{ST} values, in contrast to the RB3LYP results, showing that the spin crossover based on RB3LYP calculations is not real and that electron correlation is critical for the π-dimers with D larger than 3.3 Å. The RB3LYP calculations are incomplete, and the "spin crossover" of a molecular dimer[36d,58,59] should rather be explained by a switch between delocalization and localization of the two radical electrons. This behavior is analogous to the solid-state Mott transition when the bandwidth W decreases while U remains constant.[60] We further performed stability analyses for the RB3LYP singlet wave functions for all structures in Table 2. We obtained exactly the same results for total energies and $\langle S^2\rangle$ values as those from direct UB3LYP calculations, providing further evidence for the correctness of our UB3LYP results.

Recent UB3LYP calculations on ethyl-SBP (173 K structure) by Taniguchi et al.[61] obtained a ferromagnetic interaction ($\Delta E_{ST} = 0.032$ eV) for a "non-π-dimer pair", which refers to a pair of molecules between neighboring π-dimers. The distance between these two SBPs in the "non-π-dimer pair" and the oblique orientation of the π-orbitals would indicate that the corresponding t values are small. Nevertheless, this finding raises a question to the π-dimer approach used in this paper. If such a strong ferromagnetic coupling indeed exists among the various SBP molecules, then the dimer model and the analysis based on the Bleaney−Bowers fit of the susceptibility may be called into question. The calculations by Taniguchi et al.[61] included a correction factor based on the $\langle S^2\rangle$ values in addition to the total energies of the two states. The ΔE_{ST} thus obtained for the two high-T phase π-dimer structures of ethyl-SBP were −0.033 and −0.031 eV, almost two times larger than our values calculated directly from the total energies, which agree with those obtained from the Bleaney−Bowers dimer model fit. Our calculations reproduced their results for the π-dimers when $\langle S^2\rangle$ values are included as they did, but we could not reproduce the ferromagnetic interaction for the "non-π-dimer pair". Our calculated ΔE_{ST} for the "non-π-dimer pair" is virtually 0 eV using the same methodology as that for the π-dimers, indicating that the interdimer interaction is negligible. It appears that the Bleaney−Bowers dimer model is applicable for the high-T phase since

the R^2 value of the high-T phase fit is as good as that of the low-T phase fit. Taking the strong ferromagnetic interaction at face value, and in light of its relatively large calculated value of $\Delta E_{ST} = 0.032$ eV as compared to their antiferromagnetic counterpart, the value of $\chi_p T$ should be larger than the limiting high-T $S = 1/2$ value of 3/8 emu K mol^{-1}. This is not found in the experiment. We conclude that the calculated ferromagnetic interaction might be an artifact in ref 61.

However, the calculations for the antiferromagnetic coupling also have limitations especially for large values of the interplanar separation, D. In the propyl- and pentyl-SBP cases, although UB3LYP provides the correct sign for ΔE_{ST}, the agreement with the experimental Bleaney−Bowers fit is poor. This discrepancy indicates that one should employ higher order post-HF calculations instead of UB3LYP to account for the subtle correlation effects, although such calculations are prohibitively expensive and therefore not practical for the SBP radical dimers today.

Nevertheless, our UB3LYP calculations allow us to reach conclusions on the bonding character between the SBP radicals. For π-dimers with D shorter than 3.2 Å, restricted MO (single configuration approximation) is appropriate, and the two radical electrons are partially delocalized in the bonding HOMO. The radicals in the π-dimers can be described as being bound together by covalent $\pi-\pi$ bonding interactions. For intermediate distances in the 3.2 Å $< D <$ 3.4 Å region, the mixing of the doubly excited configuration S_2 into the ground state S_0 leads to the two electrons partially localized in the two SOMOs producing a biradical character as shown by the gradually increasing $\langle S^2 \rangle$ values with increasing D. π-Dimers in such cases can be described as open-shell singlet. For these π-dimers, there is still a certain degree of delocalization, and the $\pi-\pi$ bonding interactions still exist in the π-dimers. In the case of $D = 3.51$ Å, which is larger than the sum of the vdW radii, the two electrons are more localized on the two radicals and correlation plays a significant role. This creates a limiting case where the π-dimer may be better described by an antiferromagnetic Heisenberg exchange interaction associated with the Heisenberg spin Hamiltonian[23] as shown by the much smaller calculated ΔE_{ST} as compared to those of the other π-dimers.

The accurate estimate of ΔE_{ST} for pentyl-SBP π-dimer is challenging. The packing motif for the pentyl-SBP shown in Figure 1 indicates that the spin-bearing carbon atoms are not right on top of each other leading to a very small transfer integral (t_π). This is illustrated in Figure 11 where it is compared to other SBP systems. The cyclohexyl-SBP forms a π-chain instead of a π-dimer, but its t_π value[62] at $D = 3.28$ Å is also included for comparison. The dependence of the transfer integrals on D is generally found to be close to exponential in a wide D (2.7−3.5 Å) region.[45,63] The π-dimers of **1** and of the SBP radicals follow the exponential relationship between t_π and D with the exception of pentyl-SBP at $D = 3.51$ Å. The SBP dimer curve is lower than the phenalenyl dimer curve simply because of the normalization factor and the fact that the orbitals in SBP contain small contributions from the spiro-linkages as well.

The calculated ΔE_{ST} values of all these π-dimer structures are plotted as a function of t_π in Figure 12 and analyzed with the aid of eq 36. On the basis of our discussion of the two-site systems, we employ only the RB3LYP/RPW91 combination for these four-site systems. In Figure 12, we also provided four theoretical $\Delta E_{ST}(t_\pi)$ curves corresponding to four different values of U. The t_s values are about 0.23 eV and were obtained from dimer calculations[64] and from solid-state calculations.[22a] The intercept is at $U/4$. From this, we obtain U values in the range of 1.6−2.7 eV. The experimental and two-site U values are close

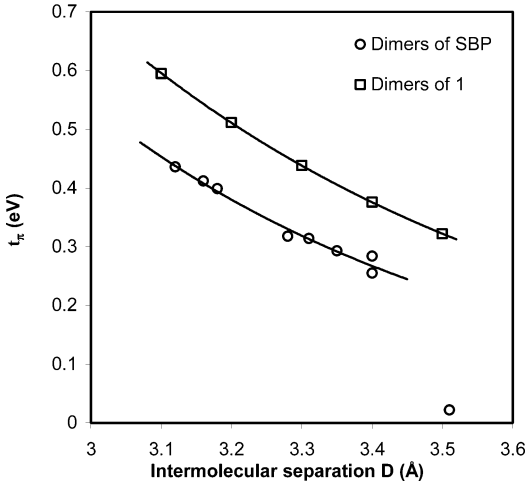

Figure 11. Transfer integrals t_π as a function of intermolecular separation D for the π-dimers of **1**, **3**−**6**, **9**, and **10** showing the nearly exponential relationship between t_π and D. The t_π value of the cyclohexyl-SBP **10** at $D = 3.28$ Å comes from the analysis of the band structure on the basis of 1D Hückel model[22a] at several reciprocal points.[62] The data point of pentyl-SBP at $D = 3.51$ Å does not follow the exponential trend, and the t_π value is nearly zero. Note the large parallel offset for pentyl-SBP; see Figure 1.

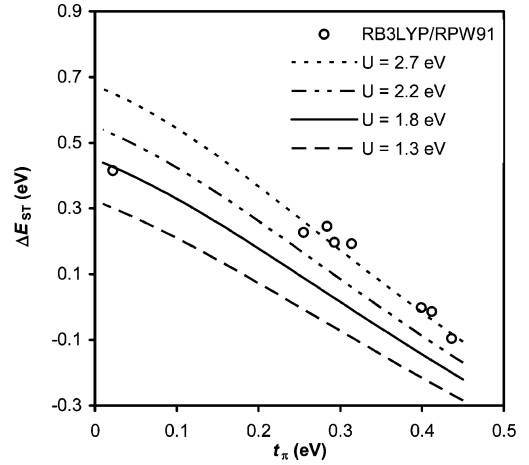

Figure 12. ΔE_{ST} as a function of t_π for the π-dimerized SBP radicals calculated with the RB3LYP/RPW91 approach, which refers to a combination of RB3LYP for ΔE_{ST} and RPW91for t_π. The various lines are from eq 36, with $t_s = 0.23$ eV, and four U values as indicated. Data points refer to dimers of SBPs with the following substituents from left to right: pentyl, propyl, octyl, ethyl (293, 173, 100, and 20 K), and butyl (173 K).

to the lower end of this range. During the derivation eq 36, we only used two SOMO-derived orbitals out of the four available and we neglected many terms other than the on-site Coulomb integrals leading to a rather crude general relationship between ΔE_{ST} and t_π.

5. Conclusions

Magnetism is related to chemical bonding through the antiferromagnetic coupling of a pair of electrons. On one hand, the exchange interaction between spins can be viewed as the borderline case of a very weak chemical bonding, and on the other hand, a regular single bond can be viewed as an extreme case of antiferromagnetic coupling. This understanding has been well-accepted[23,26] and is applicable to the $\pi-\pi$ bonding of organic π-radicals as well. The SOMO−SOMO overlap is the driving force of such covalent $\pi-\pi$ bonding, which brings the two radical molecules slightly closer together than the sum of

the vdW radii. The singlet−triplet splittings ΔE_{ST} can be used as a measure of bonding strength.[35,49]

In this paper, we have presented a theoretical framework for two-site and four-site π-dimer systems on the basis of restricted MO theory. We have investigated the bonding characteristics of the π-dimers of 2,5,8-tri-*tert*-butylphenalenyl organic radical (**2**) and a series of SBP neutral radicals (**3**−**6** and **9**) with the observed wide range of intermolecular separation $3.12 < D < 3.51$ Å. Paramagnetic susceptibilities of the π-dimerized SBP radicals have been analyzed using the Bleaney−Bowers dimer model. Restricted and unrestricted DFT calculations and wave function stability calculations have been performed to compare the calculated ΔE_{ST} values with those obtained from magnetic properties. When D is in the lower portion of the observed range of 3.12−3.51 Å, the calculated ΔE_{ST} values by the hybrid DFT B3LYP are semiquantitative, when a Hubbard dimer model can be approximated by restricted MO theory capturing the essence of the relatively large singlet−triplet splitting and the partially delocalized electron pair in the bonding HOMO. For D values above the Coulson−Fisher point, the unrestricted solutions are different from the restricted ones. The unrestricted calculations provided an economical way to partially account for electron correlation of the singlet ground state as a function of the strength of the interradical interaction.

For all of the π-dimers in this study, we conclude that with the increasing of intermolecular separation D the bonding interactions in the π-dimers are gradually weakened with a qualitative change occurring around 3.2−3.3 Å. For the π-dimers with intermolecular separations $3.3 < D < 3.4$ Å, there is still a significant part of intermolecular covalent $\pi-\pi$ bonding interaction contributing to the bonding of the two radicals. In the case of very weak interaction as in the π-dimer of **6** with an intermolecular separation $D = 3.51$ Å, the SOMO−SOMO overlap is weak and the transfer integral t_π is small. Eventually, the intermolecular interaction moves to the domain of Heisenberg exchange interaction as in the antiferromagnetic Heisenberg $S = 1/2$ linear chain model for the 1D π-step structure of **8**.[18] There is no clear-cut borderline where one can differentiate between Heisenberg exchange interaction of localized spins and a pair of delocalized electrons providing bonding interaction. However, the qualitative description of a transition from low D values with significant intermolecular $\pi-\pi$ bonding and electron delocalization to high D values with localized spins and biradicaloid character offers useful insights into the bonding and magnetic characteristics of these interesting molecular conductors.

The behavior of **10** is more complex than the rest of the SBPs because of the chainlike aggregation of the radicals, which is outside the scope of this paper. However, we note that the intermolecular separation of $D = 3.28$ Å for **10** falls in the range, where partial delocalization of electrons among the radicals becomes important. Such delocalization must play a key role in the high conductivity of **10**.[20,22]

Acknowledgment. We are deeply indebted to Dr. M. E. Itkis and Prof. R. C. Haddon for providing the magnetic data. Financial support from the National Science Foundation (Grant DMR-0331710) is gratefully acknowledged.

References and Notes

(1) (a) Haddon, R. C. *Nature* **1975**, *256*, 394. (b) Haddon, R. C. *Aust. J. Chem.* **1975**, *28*, 2343. (c) In addition to phenalenyls proposed in (a) and (b), a wide range of heterocyclic thiazyl radicals (and their selenium analogues) is also in the limelight for this purpose. For a review, see (c) Rawson, J. M.; Alberola, A.; Whalley, A. *J. Mater. Chem.* **2006**, *26*, 2560.

(2) (a) Reid, D. H. *Chem. Ind.* **1956**, 1504. (b) Gerson, F. *Helv. Chim. Acta* **1966**, *49*, 1463.

(3) Zheng, S.; Lan, J.; Khan, S. I.; Rubin, Y. *J. Am. Chem. Soc.* **2003**, *125*, 5786.

(4) (a) Goto, K.; Kubo, T.; Yamamoto, K.; Nakasuji, K.; Sato, K.; Shiomi, D.; Takui, T.; Kubota, M.; Kobayashi, T.; Takusi, K.; Ouyang, J. *J. Am. Chem. Soc.* **1999**, *121*, 1619. (b) Fukui, K.; Sato, K.; Shiomi, D.; Takui, T.; Itoh, K.; Gotoh, K.; Kubo, T.; Yamamoto, K.; Nakasuji, K.; Naito, A. *Synth. Met.* **1999**, *103*, 2257.

(5) Suzuki, S.; Morita, Y.; Fukui, K.; Sato, K.; Shiomi, D.; Takui, T.; Nakasuji, K. *J. Am. Chem. Soc.* **2006**, *128*, 2530.

(6) Small, D.; Zaitsev, V.; Jung, Y.; Rosokha, S. V.; Head-Gordon, M.; Kochi, J. K. *J. Am. Chem. Soc.* **2004**, *126*, 13850.

(7) Takano, Y.; Taniguchi, T.; Isobe, H.; Kubo, T.; Morita, Y.; Yamamoto, K.; Nakasuji, K.; Takui, T.; Yamaguchi, K. *J. Am. Chem. Soc.* **2002**, *124*, 11122.

(8) (a) Small, D.; Rosokha, S. V.; Kochi, J. K.; Head-Gordon, M. *J. Phys. Chem. A* **2005**, *109*, 11261. (b) Zaitsev, V.; Rosokha, S. V.; Head-Gordon, M.; Kochi, J. K. *J. Org. Chem.* **2006**, *71*, 520.

(9) Lü, J.-M.; Rosokha, S. V.; Kochi, J. K. *J. Am. Chem. Soc.* **2003**, *125*, 12161.

(10) Devic, T.; Yuan, M.; Adams, J.; Fredrickson, D. C.; Lee, S.; Venkataraman, D. *J. Am. Chem. Soc.* **2005**, *127*, 14616.

(11) (a) Novoa, J. J.; Lafuente, P.; Del Sesto, R. E.; Miller, J. S. *Angew. Chem., Int. Ed.* **2001**, *40*, 2540. (b) Del Sesto, R. E.; Miller, J. S.; Lafuente, P.; Novoa, J. J. *Chem. Eur. J.* **2002**, *8*, 4894. (c) Jakowski, J.; Simons, J. *J. Am. Chem. Soc.* **2003**, *125*, 16089. (d) Jung, Y.; Head-Gordon, M. *Phys. Chem. Chem. Phys.* **2004**, *6*, 2008. (e) For a review on $[TCNE]_2^{2-}$, see Miller, J. S.; Novoa, J. J. *Acc. Chem. Res.* **2007**, *40*, 189.

(12) (a) Brocks, G. *J. Chem. Phys.* **2000**, *112*, 5353. (b) Sakai, T.; Satou, T.; Kaikawa, T.; Takimiya, K.; Otsubo, T.; Aso, Y. *J. Am. Chem. Soc.* **2005**, *127*, 8082. (c) Scherlis, D. A.; Marzari, N. *J. Phys. Chem. B* **2004**, *108*, 17791.

(13) (a) For $[TCNB]_3^{2-}$, see Bagnato, J. D.; Shum, W. W.; Strohmeier, M.; Grant, D. M.; Arif, A. M.; Miller, J. S. *Angew. Chem., Int. Ed.* **2006**, *45*, 5326−5331. (b) For $[RCN_2S_2]_3^+$, see Bryan, C. D.; Cordes, A. W.; Haddon, R. C.; Hicks, R. G.; Oakley, R. T.; Palstra, T. T. M.; Perel, A. S.; Scott, S. R. *Chem. Mater.* **1994**, *6*, 508.

(14) Ethyl- and butyl-SBPs: (a) Chi, X.; Itkis, M. E.; Kirschbaum, K.; Pinkerton, A. A.; Oakley, R. T.; Cordes, A. W.; Haddon, R. C. *J. Am. Chem. Soc.* **2001**, *123*, 4041. (b) Itkis, M. E.; Chi, X.; Cordes, A. W.; Haddon, R. C. *Science* **2002**, *296*, 1443. (c) Chi, X.; Tham, F. S.; Cordes, A. W.; Itkis, M. E.; Haddon, R. C. *Synth. Met.* **2003**, *133*−*134*, 367.

(15) Propyl-SBP: Chi, X.; Itkis, M. E.; Reed, R. W.; Oakley, R. T.; Cordes, A. W.; Haddon, R. C. *J. Phys. Chem. B* **2002**, *106*, 8278.

(16) Pentyl-SBP: Chi, X.; Itkis, M. E.; Tham, F. S.; Oakley, R. T.; Cordes, A. W.; Haddon, R. C. *Int. J. Quant. Chem.* **2003**, *95*, 853.

(17) Hexyl-SBP: Chi, X.; Itkis, M. E.; Patrick, B. O.; Barclay, T. M.; Reed, R. W.; Oakley, R. T.; Cordes, A. W.; Haddon, R. C. *J. Am. Chem. Soc.* **1999**, *121*, 10395.

(18) Benzyl-SBP: Pal, S. K.; Itkis, M. E.; Reed, R. W.; Oakley, R. T.; Cordes, A. W.; Tham, F. S.; Siegrist, T.; Haddon, R. C. *J. Am. Chem. Soc.* **2004**, *126*, 1478.

(19) Octyl-SBP: Liao, P.; Itkis, M. E.; Oakley, R. T.; Tham, F. S.; Haddon, R. C. *J. Am. Chem. Soc.* **2004**, *126*, 14297.

(20) Cyclohexyl-SBP: Pal, S. K.; Itkis, M. E.; Tham, F. S.; Reed, R. W.; Oakley, R. T.; Haddon, R. C. *Science* **2005**, *309*, 281.

(21) In addition to π-dimerization, **9** also forms a σ-dimerized polymorph similar to **1** (ref 19).

(22) (a) Huang, J.; Kertesz, M. *J. Am. Chem. Soc.* **2006**, *128*, 1418. (b) Böhlin, J.; Hansson, A.; Stafström, S. *Phys. Rev. B* **2006**, *74*, 155111.

(23) (a) Itoh, K., Kinoshita, M., Eds. *Molecular Magnetism*−*New Magnetic Materials*; Kodansha Ltd., Gordon and Beach Science Publishers: Tokyo and Amsterdam, 2000. (b) Veciana, J.; Ed. *π-Electron Magnetism from Molecules to Magnetic Materials*; Springer- Verlag: Berlin, 2001.

(24) Transfer integral t is used interchangeably with Hückel resonance integral β.

(25) Borden, W. T., Ed. *Diradicals*; John Wiley & Sons: New York, 1982.

(26) Theoretical approaches based on natural and orthogonalized magnetic orbitals are also feasible. See Kahn, O. *Molecular Magnetism*; VCH Publishers: New York, 1993.

(27) Szabo, A.; Ostlund, N. S. *Modern Quantum Chemistry-Introduction to Advanced Electronic Structure Theory*; Dover Publications, Inc.: Mineola, NY, 1996.

(28) Within the context of the Hubbard model, in the large $U/4t$ limit, the two ^1A_g configurations mix strongly, giving rise to correlation effects. In the small $U/4t$ limit, there is little mixing and these configurations are quite accurate.

(29) Morita, Y.; Aoki, T.; Fukui, K.; Nakazawa, S.; Tamaki, K.; Suzuki, S.; Fuyuhiro, A.; Yamamoto, K.; Sato, K.; Shiomi, D.; Naito, A.; Takui, T.; Nakasuji, K. *Angew. Chem., Int. Ed.* **2002**, *41*, 1793.

(30) Kubo, T.; Shimizu, A.; Sakamoto, M.; Uruichi, M.; Yakushi, K.; Nakano, M.; Shiomi, D.; Sato, K.; Takui, T.; Morita, Y.; Nakasuji, K. *Angew. Chem., Int. Ed.* **2005**, *44*, 6564.

(31) (a) Noodleman, L.; Baerends, E. J. *J. Am. Chem. Soc.* **1984**, *106*, 2316. (b) McManus, G. D.; Rawson, J. M.; Feeder, N.; van Duijn, J.; McInnes, E. J. L.; Novoa, J. J.; Burriel, R.; Palacio, F.; Oliete, P. *J. Mater. Chem.* **2001**, *11*, 1992. (c) Polo, V.; Kraka, E.; Cremer, D. *Theor. Chem. Acc.* **2002**, *107*, 291.

(32) Soos, Z. G.; Bondeson, S. R. In *Extended Linear Chain Compounds*; Miller, J. S., Ed.; Plenum Press: New York, 1983; Vol. 3, pp 196−197.

(33) (a) Tanner, D. B.; Miller, J. S.; Rice, M. J.; Ritsko, J. J. *Phys. Rev. B* **1980**, *21*, 5835. (b) Torrance, J. B.; Scott, B. A.; Welber, B.; Kaufman, F. B.; Seiden, P. E. *Phys. Rev. B* **1979**, *19*, 730. (c) Miller, L. L.; Mann, K. R. *Acc. Chem. Res.* **1996**, *29*, 417.

(34) Tanner, D. B. In *Extended Linear Chain Compounds*; Miller, J. S., Ed.; Plenum Press: New York, 1983; Vol. 2, p 205.

(35) Rajca, A. *Chem. Rev.* **1994**, *94*, 871.

(36) (a) Harris, A. B.; Lange, R. V. *Phys. Rev.* **1967**, *157*, 295. (b) Rice, M. J. *Solid State Commun.* **1979**, *31*, 93. (c) Pincus, P. In *Selected Topics in Physics, Astrophysics, and Biophysics*; Abecassis de Laredo, E., Jurisic, N. K., Eds.; D. Reidel Publishing Co.: Dordrecht-Holland, The Netherlands, 1973; p 152. (d) Whangbo, M.-H. *J. Chem. Phys.* **1979**, *70*, 4963.

(37) Matlak, M.; Aksamit, J.; Grabiec, B.; Nolting, W. *Ann. Phys. (Leipzig)* **2003**, *12*, 304.

(38) Strongly-correlated systems have $U \gg W$; see Fulde, P. *Electron Correlations in Molecules and Solids*, 3rd ed.; Springer-Verlag: Berlin, Germany, 1995; p 281.

(39) Frisch, M. J.; Trucks, G. W.; Schlegel, H. B.; Scuseria, G. E.; Robb, M. A.; Cheeseman, J. R.; Montgomery, J. A., Jr.; Vreven, T.; Kudin, K. N.; Burant, J. C.; Millam, J. M.; Iyengar, S. S.; Tomasi, J.; Barone, V.; Mennucci, B.; Cossi, M.; Scalmani, G.; Rega, N.; Petersson, G. A.; Nakatsuji, H.; Hada, M.; Ehara, M.; Toyota, K.; Fukuda, R.; Hasegawa, J.; Ishida, M.; Nakajima, T.; Honda, Y.; Kitao, O.; Nakai, H.; Klene, M.; Li, X.; Knox, J. E.; Hratchian, H. P.; Cross, J. B.; Bakken, V.; Adamo, C.; Jaramillo, J.; Gomperts, R.; Stratmann, R. E.; Yazyev, O.; Austin, A. J.; Cammi, R.; Pomelli, C.; Ochterski, J. W.; Ayala, P. Y.; Morokuma, K.; Voth, G. A.; Salvador, P.; Dannenberg, J. J.; Zakrzewski, V. G.; Dapprich, S.; Daniels, A. D.; Strain, M. C.; Farkas, O.; Malick, D. K.; Rabuck, A. D.; Raghavachari, K.; Foresman, J. B.; Ortiz, J. V.; Cui, Q.; Baboul, A. G.; Clifford, S.; Cioslowski, J.; Stefanov, B. B.; Liu, G.; Liashenko, A.; Piskorz, P.; Komaromi, I.; Martin, R. L.; Fox, D. J.; Keith, T.; Al-Laham, M. A.; Peng, C. Y.; Nanayakkara, A.; Challacombe, M.; Gill, P. M. W.; Johnson, B.; Chen, W.; Wong, M. W.; Gonzalez, C.; Pople, J. A. *Gaussian 03*, revision B.04; Gaussian, Inc.: Wallingford, CT, 2004.

(40) (a) Perdew, J. P.; Wang, Y. *Phys. Rev. B* **1992**, *45*, 13244. (b) Perdew, J. P.; Chevary, J. A.; Vosko, S. H.; Jackson, K. A.; Peterson, M. R.; Singh, D. J.; Fiolhais, C. *Phys. Rev. B* **1992**, *46*, 6671.

(41) (a) Becke, A. D. *Phys. Rev. A* **1988**, *38*, 3098. (b) Lee, C.; Yang, W.; Parr, R. G. *Phys. Rev. B* **1988**, *37*, 785.

(42) Becke, A. D. *J. Chem. Phys.* **1993**, *98*, 5648.

(43) Bauernschmitt, R.; Ahlrichs, R. *J. Chem. Phys.* **1996**, *104*, 9047.

(44) (a) Kresse, G.; Furthmüller, J. *Phys. Rev. B* **1996**, *54*, 11169. (b) Kresse, G.; Hafner, J. *Phys. Rev. B* **1993**, *47*, 558. (c) Using Vanderbilt type (Vanderbilt, D. *Phys. Rev. B* **1990**, *41*, 7892) ultrasoft pseudopotentials (Kresse, G.; Hafner, J. *J. Phys.*: *Condens. Matter* **1994**, *6*, 8245).

(45) Huang, J.; Kertesz, M. *J. Chem. Phys.* **2005**, *122*, 234707.

(46) Huang, J.; Kertesz, M. *Chem. Phys. Lett.* **2004**, *390*, 110.

(47) (a) Mitani, M.; Mori, H.; Takano, Y.; Yamaki, D.; Yoshioka, Y.; Yamaguchi, K. *J. Chem. Phys.* **2000**, *113*, 4035. (b) Saito, T.; Ito, A.; Tanaka, K. *J. Phys. Chem. A* **1998**, *102*, 8021.

(48) (a) Gogonea, V.; Schleyer, P. v. R.; Schreiner, P. R. *Angew. Chem., Int. Ed.* **1998**, *37*, 1945. (b) Ito, A.; Ino, H.; Ichiki, H.; Tanaka, K. *J. Phys. Chem. A* **2002**, *106*, 8716. (c) Ruiz, E.; Alemany, P.; Alvarez, S.; Cano, J. *J. Am. Chem. Soc.* **1997**, *119*, 1297. (d) Wittbrodt, J. M.; Schlegel, H. B. *J. Chem. Phys.* **1996**, *105*, 6574.

(49) Michl, J. *Acc. Chem. Res.* **1990**, *23*, 127.

(50) Huang, J.; Kertesz, M. *J. Am. Chem. Soc.* **2006**, *128*, 7277.

(51) (a) Garito, A. F.; Heeger, A. J. *Acc. Chem. Res.* **1974**, *7*, 232. (b) Torrance, J. B. *Acc. Chem. Res.* **1979**, *12*, 79.

(52) Haddon, R. C.; Wudl, F.; Kaplan, M. L.; Marshall, J. H.; Cais, R. E.; Bramwell, F. B. *J. Am. Chem. Soc.* **1978**, *100*, 7629.

(53) (a) Koutentis, P. A.; Chen, Y.; Cao, Y.; Best, T. P.; Itkis, M. E.; Beer, L.; Oakley, R. T.; Cordes, A. W.; Brock, C. P.; Haddon, R. C. *J. Am. Chem. Soc.* **2001**, *123*, 3864. (b) Zheng, S.; Thompson, J. D.; Tontcheva, A.; Khan, S. I.; Rubin, Y. *Org. Lett.* **2005**, *7*, 1861.

(54) Dorfman, Ya. G. *Diamagnetism and the Chemical Bond*; American Elsevier Publishing Co., Inc.: New York, 1965.

(55) Lahti, P. M., Ed. *Magnetic Properties of Organic Materials*; Marcel Dekker, Inc.: New York, 1999; p 558.

(56) Escuer, A.; Kumar, S. B.; Font-Bardía, M.; Solans, X.; Vicente, R. *Inorg. Chim. Acta* **1999**, *286*, 62.

(57) The correct value of the constant is 1.604 and not the widely used 1.599 as in ref 26.

(58) Whangbo, M.-H. In *Extended Linear Chain Compounds*; Miller, J. S., Ed.; Plenum Press: New York, 1983; Vol. 2, p 136.

(59) Huang, J.; Kertesz, M. *J. Am. Chem. Soc.* **2003**, *125*, 13334.

(60) Fazekas, P. *Lecture Notes on Electron Correlation and Magnetism*; World Scientific: Singapore, 1999; p 147 ff.

(61) Taniguchi, T.; Kawakami, T.; Yamaguchi, K. *Polyhedron* **2005**, *24*, 2274.

(62) (a) The analysis of the band structure at only the Γ point gives $t_\pi = 0.27$ eV (ref 22a). (b) A more accurate value can be obtained by averaging over several reciprocal points; see Huang, J. Georgetown University Ph.D. dissertation, 2006; Chapter 9.

(63) (a) Senthikumar, K.; Grozema, F. C.; Bickelhaupt, F. M.; Siebbeles, L. D. A. *J. Chem. Phys.* **2003**, *119*, 9809. (b) Brédas, J. L.; Calbert, J. P.; da Silva Filho, D. A.; Cornil, J. *Proc. Natl. Acad. Sci. U.S.A.* **2002**, *99*, 5804.

(64) t_s of the SBP radicals are, in the order of increasing D shown in Table 2: 0.227, 0.230, 0.227, 0.240, 0.234, 0.235, 0.239, and 0.199 eV, respectively. The variations are due to differences in geometries and substituents.